Angular and polarization correlations in photoionization and radiative recombination

James H. Scofield
Theoretical Atomic Physics Group, Lawrence Livermore National Laboratory, Livermore, California 94550
(Received 27 March 1989)

The relativistic formulation is given for the angular distribution of the electrons produced in the photoionization by linearly polarized photons and the distribution of photons of a particular polarization produced in the inverse process of radiative recombination. The electrons are treated as moving in a self-consistent Hartree-Slater central potential. Results are given for the radiative recombination onto heliumlike nickel and neonlike barium for electrons in the energy range below 100 keV.

I. INTRODUCTION

At nonrelativistic energies, the photoionization cross sections and the inverse process of radiative recombination are dominated by electric dipole transitions and the angular distribution of the ejected electron is specified by a single parameter. For linearly polarized radiation the cross section is a function of the angle between the x-ray polarization direction and the electron's direction. As the energy is increased, higher multipoles contribute and the distribution is also dependent on the direction of the incoming photon. In general, the electron is ejected preferentially in the direction of the incoming photon.

In the present treatment, I wish to look at the electron angular distribution resulting from a plane-polarized incoming photon beam. The main emphasis is on the region from 1 to 100 keV. Detailed examples of theoretical calculations of the electron angular correlations for unpolarized radiation have previously been given.[1] The few examples looking at the relativistic effects with linear polarization have been aimed at energies in the MeV region.[2] The radiation emitted by synchrotrons is polarized. Angular correlation experiments in the kilovolt range should be feasible in showing relativistic effects and they should be taken into account in interpreting experimental results in the energy range above a few kilovolts. Recent experiments[3] have observed the x rays emitted at a particular angle in the capture of electrons from a beam incident on highly stripped ions. The radiative capture process has been used to normalize the electron-impact-excitation cross sections measured in these experiments. The measurement of the polarization of the radiative recombination emission is being explored.[4] This paper is designed to present examples of calculations pertinent to these experiments measuring the radiative recombination radiation in the case of He-like nickel and Ne-like barium.

II. THEORY

The presentation is given here in terms of the photoionization process. The radiative capture and photoionization processes are the inverse of each other. In the radiative capture process, the electrons enter asymptotically with plane waves; in photoionization they are measured in final plane-wave states. In principle, the phase shifts enter with opposite signs for the two processes. However, the overall sign of the phase shifts do not enter the results.

The present treatment will use an independent-particle description of the electrons. In addition to errors in such a theory due to inaccuracies in the bound-state wave functions, there are corrections for low-energy outgoing electrons due to explicit dependence of the electron on its coupling with the ion. There are also major corrections to the independent-particle model in resonance regions in which collective motions of the electrons must be taken into account.

In regions away from edges, the independent-particle model is very accurate in giving the total cross sections[5] and should be suitable, in its range of validity, in treating the angular factors.

The relativistic theory for the photoionization of electrons in a central potential has been given several times before.[6–10] The general formulation contains all of the correlations between the incoming photons and outgoing photoelectrons. In this paper, I wish to examine the angular dependence of the ejected electron resulting from an incoming plane-polarized photon beam. The dependence of the cross sections on the spin of the electrons is not included. The maintenance of the expressions in terms of the reduced matrix elements for the multipole transitions allows a simplicity to the expressions not fully displayed before.

The process consists in a plane-wave beam of photons coming in, ejecting a bound electron, and a free electron going out. The basic matrix element is given as

$$M=(\psi^{\dagger}(\mathbf{p})|\boldsymbol{\alpha}\cdot\boldsymbol{\epsilon}\exp(i\mathbf{k}\cdot\mathbf{r})|\psi_0)\ , \tag{1}$$

in which ψ_0 is a bound solution of the Dirac equation, $\mathbf{k}$ and $\boldsymbol{\epsilon}$ are the wave number and polarization of the photon, and $\psi(\mathbf{p})$ is the free-electron solution that goes as an outgoing plane wave at large distances.

The matrix element is evaluated by specifying the photons as moving in the z direction. The coordinate system used for the calculation is shown in Fig. 1. The radiation is expanded in electric and magnetic multipole moments:[11]

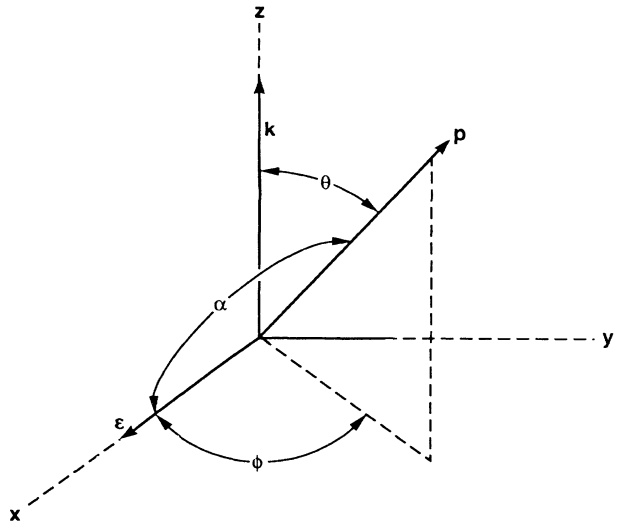

FIG. 1. Coordinate system with the photon momentum k, polarization ϵ, and electron momentum p.

$$\mathbf{e}_\mu \exp(i\mathbf{k}\cdot\mathbf{r}) = -\sum_L [(2L+1)/8\pi]^{1/2} \times [\mathbf{A}^{(e)}_{L\mu}(k,\mathbf{r}) + \mu \mathbf{A}^{(m)}_{L\mu}(k,\mathbf{r})] \ . \tag{2a}$$

The vectors $\mathbf{e}_\mu$ are the spherical unit vectors, and

$$\mathbf{A}^{(e)}_{L\mu}(k,r) = i^L [L(L+1)]^{-1/2} k^{-1} \nabla \times \mathbf{L} j_L(kr) Y_{L\mu}(\hat{r}) \ , \tag{2b}$$

$$\mathbf{A}^{(m)}_{L\mu}(k,r) = i^L [L(L+1)]^{-1/2} j_L(kr) \mathbf{L} Y_{L\mu}(\hat{r}) \ . \tag{2c}$$

The four-component wave function for a bound state with total angular momentum j and orbital angular momentum l is given in terms of radial wave functions as

$$\psi = \frac{i^l}{r} \begin{bmatrix} G(r) & \chi_{\kappa m}(\hat{r}) \\ iF(r) & \chi_{-\kappa m}(\hat{r}) \end{bmatrix} \ . \tag{3}$$

The relativistic angular-momentum parameter

$$\kappa = -2(j-l)(j+\tfrac{1}{2})$$

is used to label the states with l and j the orbital and total angular momentum of a state. The two-component angular-momentum states are given as

$$\chi_{\kappa m}(\hat{r}) = \sum_{m',\sigma} C(lm'\tfrac{1}{2}\sigma; jm) Y_{lm'}(\hat{r}) U_{\frac{1}{2}\sigma} \ . \tag{4}$$

The phase of the wave functions has been chosen so that the reduced matrix elements will be real.[12]

The free-electron wave function is expanded in states of definite angular momentum:

$$\psi(\mathbf{p}) = 4\pi p^{-1} \sum_{\kappa,m} [\chi^\dagger_{\kappa m}(\hat{p}) u] \chi_{\kappa m}(p,\mathbf{r}) e^{-i\delta_\kappa} \ , \tag{5}$$

in which u is the spin state of the plane-wave state at asymptotic distances. The free states $\chi_{\kappa m}$ of definite angular momentum have the same structure as the bound states. At large distances, the radial wave function for the large component goes as

$$G_\kappa(p,r) \sim [(E+mc^2)/2E]^{1/2} \times \sin[pr + \tfrac{1}{2} l\pi + \eta \ln(pr) + \delta_\kappa] \ , \tag{6}$$

in which E is the total energy of the electron.

The parameter η is given by

$$\eta = Z_i \alpha E / p$$

in which Z_i is the charge of the ion. We sum here over the spin of the electrons and average over their initial magnetic sublevels. There is then a dependence only on the linear polarization of the photons.

The total cross section for photoionization from a given subshell is given by

$$\sigma = [16\pi^2 \alpha E N / (2j_0+1)\omega p] \sum_{\kappa,L,\pi} |\langle \kappa \| A^\pi_L \| \kappa_0 \rangle|^2 \ , \tag{7}$$

in which N is the number of electrons in the subshell. The sum over π indicates the sum over the electric and magnetic components.

The differential cross section for the ejection of an electron with an angle θ from the photon direction and an azimuthal angle ϕ measured from the polarization direction is given by

$$\frac{d\sigma}{d\Omega} = [4\pi\alpha E N/(2j_0+1)\omega p] \sum_{\substack{\lambda,\kappa,\kappa' \\ L,\pi,L',\pi'}} (-1)^{L+j-L'-j'+j_0+1/2} (2\lambda+1)(j,j',l,l',L,L')^{1/2} \times \cos(\delta_{\kappa'} - \delta_\kappa) \begin{bmatrix} l & l' & \lambda \\ 0 & 0 & 0 \end{bmatrix} \begin{Bmatrix} l & l' & \lambda \\ j' & j & \frac{1}{2} \end{Bmatrix} \begin{Bmatrix} j & j' & \lambda \\ L' & L & j_0 \end{Bmatrix} \langle \kappa \| A^\pi_L \| \kappa_0 \rangle \langle \kappa' \| A^{\pi'}_{L'} \| \kappa_0 \rangle \times \left[\begin{bmatrix} \lambda & L' & L \\ 0 & 1 & -1 \end{bmatrix} P_\lambda(\cos\theta) - (-1)^{l'-L'-l_0} \begin{bmatrix} \lambda & L' & L \\ 2 & -1 & -1 \end{bmatrix} \times \left[\frac{(\lambda-2)!}{(\lambda+2)!} \right]^{1/2} P^{(2)}_\lambda(\cos\theta)\cos(2\phi) \right] \ . \tag{8}$$

The symbol $(a,b,\ldots)$ denotes the product $(2a+1)(2b+1)\ldots$. The angular functions, P_λ and $P^{(2)}_\lambda$, are the Legendre

and associated Legendre functions, respectively.

The reduced matrix elements are given by

$$\langle \kappa m | A^{(\pi)}_{L\mu} | \kappa_0 m \rangle = (-1)^{L-j_0+j}(2j+1)^{-1/2} C(L\mu j_0 m_0; jm) \langle \kappa \| A^{\pi}_{L} \| \kappa_0 \rangle \tag{9}$$

and have the explicit expressions in terms of the radial matrix elements:

$$\langle \kappa \| A^{e}_{L} \| \kappa_0 \rangle = -(-1)^{1/2(L+l_0-l)}(4\pi)^{-1/2} b(\kappa,\kappa_0,L) R^{e}_{L} , \tag{10a}$$

$$\langle \kappa \| A^{m}_{L} \| \kappa_0 \rangle = -(-1)^{1/2(L+1+l_0-l)}(4\pi)^{-1/2} b(\kappa,-\kappa_0,L) R^{m}_{L} , \tag{10b}$$

with

$$b(\kappa,\kappa_0,L) = (-1)^{L+j_0+1/2}[(j_0,j,l_0,l,L)/L(L+1)]^{1/2} \begin{Bmatrix} L & j_0 & j \\ \frac{1}{2} & l & l_0 \end{Bmatrix} \begin{bmatrix} L & l_0 & l \\ 0 & 0 & 0 \end{bmatrix} . \tag{10c}$$

The radial matrix elements are

$$R^{e}_{L} = \int dr \{(\kappa_0-\kappa)(FG_0+GF_0)[-j_{L-1}(kr)+Lj_L(kr)/kr]+L(L+1)(FG_0-GF_0)j_L(kr)/kr\} , \tag{11a}$$

$$R^{m}_{L} = (\kappa_0+\kappa)\int dr (FG_0+GF_0) j_L(kr) . \tag{11b}$$

The radiative capture cross section for a given polarization is given in terms of the photoionization cross section as

$$\sigma_{\text{rec}} = (N_v/N)(\hbar\omega/pc)^2 \sigma_{\text{ph}} , \tag{12}$$

in which N_v is the number of vacancies in the subshell prior to recombination.

The calculation of the radial matrix elements has been carried out by numerically solving the Dirac equation and numerically integrating over the product of the wave functions and spherical Bessel functions. The Hartree-Slater approximation is used for the potential with the Latter modification used in that the potential is not dropped below that for a Coulomb field in the large radial region.[13]

III. ANGULAR DISTRIBUTION RESULTS

In the case of unpolarized photons, the cross section at a given energy is a function of the angle between the incoming photon and the outgoing electron. In the case of linearly polarized photons, the cross section depends on a second function of this angle times $\cos(2\phi)$ in which ϕ is the azimuthal angle of the ejected electron with the electric vector in the x direction. The differential cross section can be given in terms of the expansion in the angular factors:

$$\frac{d\sigma}{d\Omega} = \frac{\sigma}{4\pi}\left[\sum_{\lambda=0}^{\infty} B_\lambda P_\lambda(\cos\theta) - \sum_{\lambda=2}^{\infty} \lambda^{-1}(\lambda-1)^{-1} B^{\phi}_{\lambda} P^{(2)}_{\lambda}(\cos\theta)\cos(2\phi)\right] . \tag{13}$$

The normalization of the B^{ϕ} term has been chosen so that B and B^{ϕ} are equal for the dominant $E1$ contribution. This equality for the strictly $E1$ contribution to the $\lambda=2$ terms leads to the angular factor:

$$P_2(\cos\theta) - \tfrac{1}{2}P^{(2)}_2(\cos\theta)\cos(2\phi) = -2P_2(\cos\alpha) , \tag{14}$$

in which α is the angle between the electron direction and the polarization direction. In the low-energy region, the standard notation is to use $\beta=-2B_2$ and the angular dependence is given as

$$\frac{d\sigma}{d\Omega} = \frac{\sigma}{4\pi}[1+\beta P_2(\cos\alpha)] .$$

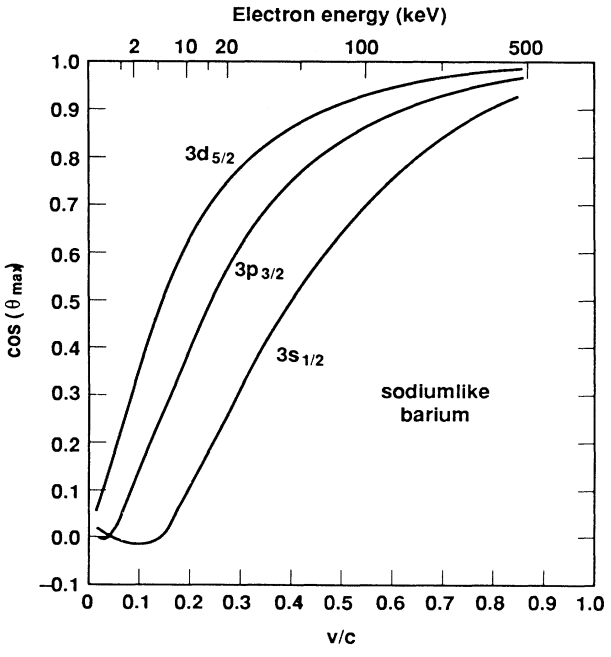

FIG. 2. Cosine of the angle for maximum electron ejection in the plane of the photon momentum and polarization as a function of the ejected electron's velocity and energy for the $n=3$ subshells of sodiumlike barium.

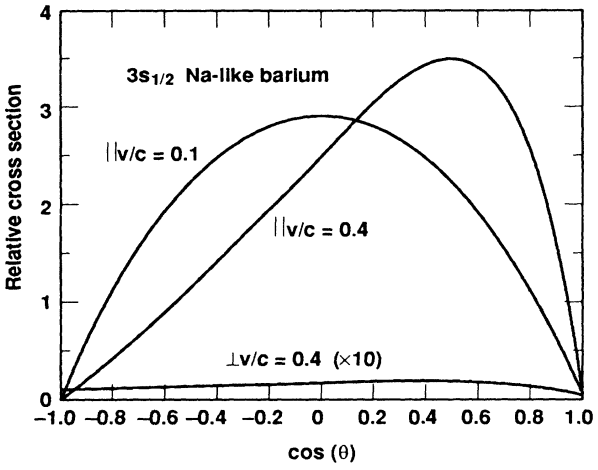

FIG. 3. Relative differential cross section for ionization from the $3s_{1/2}$ state of sodiumlike barium at v/c of 0.1 and 0.4 for the cases with the electron momentum in the photon momentum-polarization plane (||) and perpendicular to the polarization direction (⊥). The results for perpendicular electron momentum $v/c=0.1$ are close to zero.

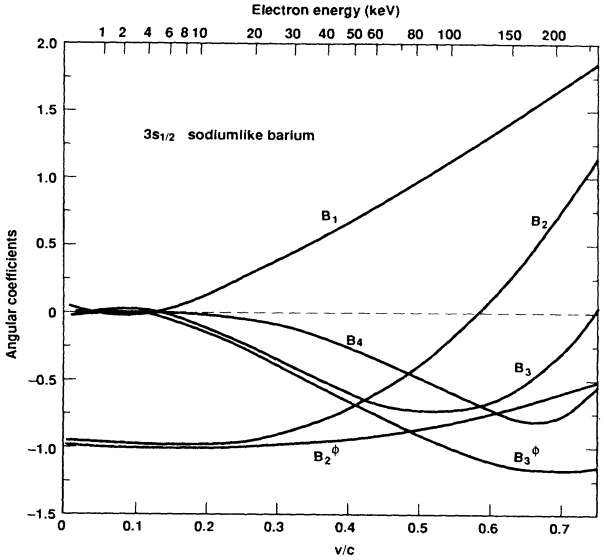

FIG. 5. The B coefficients for $\lambda=1-4$ and B^{ϕ} coefficients for $\lambda=2$ and 3 for the $3s_{1/2}$ state of sodiumlike barium.

In this low-energy region, the cross section for electrons ejected in the x-z plane ($\phi=0$) is, in general, a maximum for electrons ejected at an angle of 90° to the incoming photon's direction. For electrons in the y-z plane ($\phi=90°$) the cross section is independent of the angle between the two momenta.

As the energy is increased, the cross section is generally skewed into the forward direction. The onset of this comes in the rise of the $E2$ term. The cross terms between the $E1$ and $E2$ terms give rise to $\lambda=1$ and 3 terms which are asymmetric between backward and forward scattering. The cross sections for the s states are somewhat anomalous in that the B_1 term goes negative in the low-energy region and there is an energy range in which the cross section is skewed into the backward direction. Figure 2 shows the cosine of the angle at which the cross section for electrons ejected in the x-z plane is a maximum as a function of the ejected electron velocity for ionization from (recombination into) sodiumlike barium.

Figures 3 and 4 show the cross sections for electrons of velocities of 0.1 and 0.4 times c for sodiumlike barium in the $3s_{1/2}$ and $3d_{5/2}$ states. Shown are the differential cross sections, normalized to average unity over all directions, as a function of the angle θ between the photon and

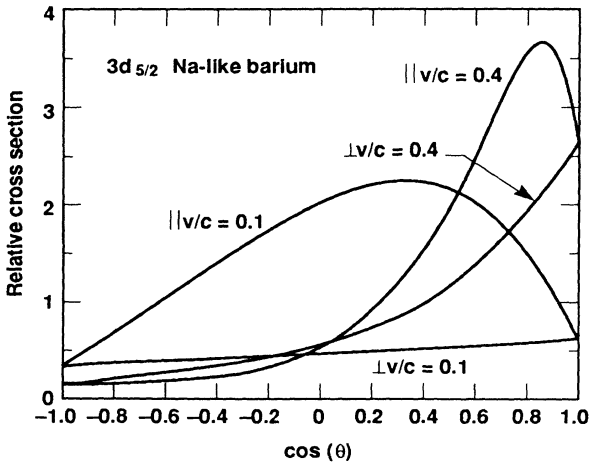

FIG. 4. Relative differential cross section for the $3d_{5/2}$ state of sodiumlike barium.

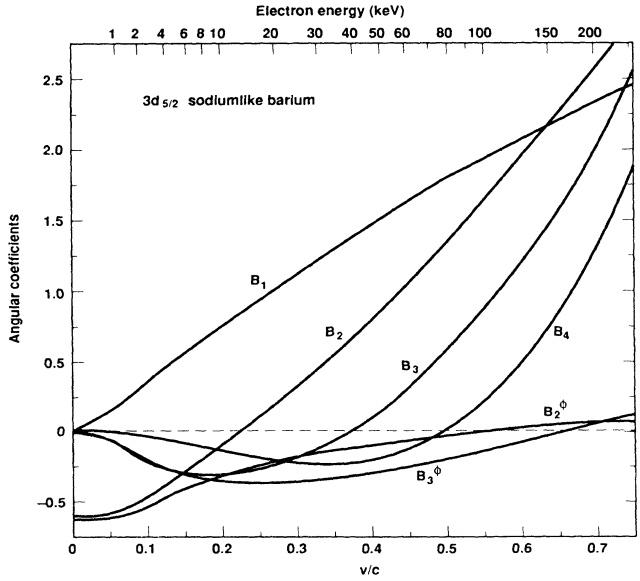

FIG. 6. The B and B^{ϕ} coefficients for the $3d_{5/2}$ state of sodiumlike barium.

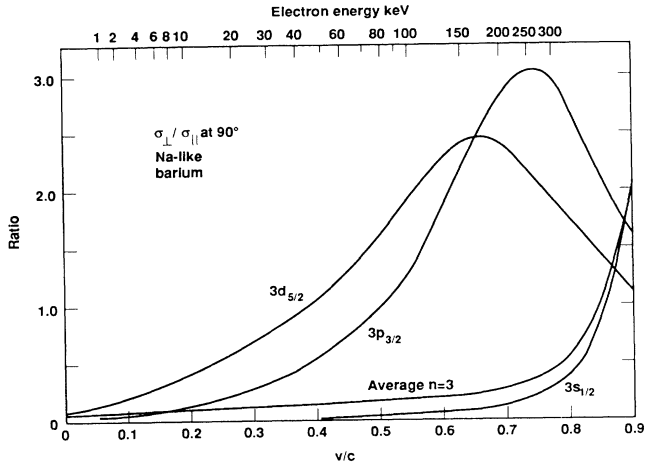

FIG. 7. The ratio of emission of x rays at $\theta=90°$ polarized perpendicular to the plane defined by the electron and photon momenta ($\phi=90°$) to that parallel to the plane ($\phi=0°$).

electron momenta. The two cases are shown; the case with the polarization vector in the plane of the two momenta ($\phi=0°$) and the case with it perpendicular to it ($\phi=90°$). For the s states, at low energies, there is little emission perpendicular to the polarization direction. For $v/c=0.1$ the normalized cross section does not exceed 7.3×10^{-3} and is not shown in Fig. 3. Even as the energy is increased, the cross section is very small.

Figures 5 and 6 show B_1-B_4, and B_2^ϕ and B_3^ϕ as a function of the electron's velocity for the $3s_{1/2}$ and $3d_{5/2}$ subshells, respectively. The curves for the other shells are very similar to these. With v/c less than 0.1 or so, only terms up through $\lambda=3$ need to be included and the B_λ and B_λ^ϕ can be taken as equal. Beyond this region the higher λ terms need to be taken into account.

For the photoionization process with electrons ejected at 90° to the photon direction, Fig. 7 shows the ratio of the cross section for electrons ejected along the y axis, i.e., perpendicular to the polarization direction, to the cross section along the x axis, i.e., parallel to the polarization direction. For the radiative recombination process with x rays emitted at 90° to the electron direction, this is the ratio of the cross section for the photon polar-

TABLE I. Radiative recombination cross sections into the $n=2$ states of heliumlike nickel.

E_e (keV)	v/c	subshell	$\hbar\omega$ (keV)	σ (b)	$d\sigma/d\Omega(90°)$ (b/sr)	$\sigma_\perp/\sigma_\parallel$
4	0.1244	$s_{1/2}$	6.404	47.85	5.663	1.79[−4][a]
		$p_{1/2}$	6.349	18.06	1.736	0.230
		$p_{3/2}$	6.325	33.90	3.275	0.234
		total		99.81	10.674	0.0973
6	0.1519	$s_{1/2}$	8.404	28.52	3.340	2.38[−4]
		$p_{1/2}$	8.349	8.385	0.766	0.285
		$p_{3/2}$	8.325	15.59	1.432	0.296
		total		52.49	5.539	0.0987
8	0.1749	$s_{1/2}$	10.404	19.26	2.230	3.07[−4]
		$p_{1/2}$	10.349	4.671	0.4085	0.334
		$p_{3/2}$	10.325	8.612	0.7573	0.353
		total		32.55	3.396	0.0971
10	0.1950	$s_{1/2}$	12.404	13.99	1.599	3.89[−4]
		$p_{1/2}$	12.349	2.900	0.2438	0.379
		$p_{3/2}$	12.325	5.309	0.4490	0.406
		total		22.20	2.291	0.0942
15	0.2371	$s_{1/2}$	17.404	7.549	0.8334	6.41[−4]
		$p_{1/2}$	17.349	1.161	0.0896	0.474
		$p_{3/2}$	17.325	2.095	0.1628	0.529
		total		10.81	1.086	0.0857
20	0.2719	$s_{1/2}$	22.404	4.735	0.5049	9.65[−4]
		$p_{1/2}$	22.349	0.585	0.0420	0.552
		$p_{3/2}$	22.325	1.043	0.0757	0.639
		total		6.364	0.6226	0.0778
50	0.4127	$s_{1/2}$	52.404	0.914	0.0784	4.51[−3]
		$p_{1/2}$	52.349	0.056	0.00280	0.954
		$p_{3/2}$	52.325	0.095	0.00491	1.344
		total		1.065	0.0862	0.556

[a] 1.79[−4] denotes 1.79×10^{-4}.

ization perpendicular to the plane of the electron and photon momenta to that with the polarization in the plane, i.e., parallel to the electron momentum.

Table I presents the total cross section for the radiative recombination into the $n=2$ states of heliumlike nickel, the total differential cross section for $\theta=90°$, and the ratio of the emission for the polarization perpendicular to the plane of the two momenta to that in the plane. Table II presents similar results for the recombination into the $n=3$ states of neonlike barium.

The results have been given here for two particular ion species which have been studied experimentally in the electron beam ion trap (EBIT) at Lawrence Livermore National Laboratory (LLNL). With a variation of the ion species the binding energies are varied as well as the total cross sections. For the limited cases studied, there

TABLE II. Radiative recombination cross sections into the $n=3$ states of neonlike barium.

E_e (keV)	v/c	subshell	$\hbar\omega$ (keV)	σ (b)	$d\sigma/d\Omega(90°)$ (b/sr)	$\sigma_\perp/\sigma_\parallel$
4	0.1244	$s_{1/2}$	7.653	61.97	7.322	2.15[−3][a]
		$p_{1/2}$	7.553	57.89	6.238	0.103
		$p_{3/2}$	7.448	103.7	11.34	0.0889
		$d_{3/2}$	7.311	35.91	3.399	0.242
		$d_{5/2}$	7.285	50.07	4.696	0.273
		total		309.54	33.00	0.107
6	0.1519	$s_{1/2}$	9.653	40.53	4.807	2.16[−3]
		$p_{1/2}$	9.553	33.77	3.547	0.121
		$p_{3/2}$	9.448	59.06	6.295	0.108
		$d_{3/2}$	9.311	16.15	1.448	0.289
		$d_{5/2}$	9.285	22.29	1.982	0.325
		total		171.8	18.08	0.112
8	0.1749	$s_{1/2}$	11.653	29.66	3.523	2.25[−3]
		$p_{1/2}$	11.553	22.35	2.284	0.139
		$p_{3/2}$	11.448	38.32	3.972	0.127
		$d_{3/2}$	11.311	8.679	0.740	0.333
		$d_{5/2}$	11.285	11.87	1.005	0.373
		total		110.9	11.52	0.116
10	0.1950	$s_{1/2}$	13.653	23.10	2.741	2.35[−3]
		$p_{1/2}$	13.553	15.90	1.582	0.156
		$p_{3/2}$	13.448	26.82	2.703	0.147
		$d_{3/2}$	13.311	5.194	0.422	0.374
		$d_{5/2}$	13.285	7.049	0.570	0.418
		total		78.06	8.017	0.118
15	0.2371	$s_{1/2}$	18.653	14.32	1.684	2.74[−3]
		$p_{1/2}$	18.553	8.163	0.7583	0.194
		$p_{3/2}$	18.448	13.31	1.251	0.194
		$d_{3/2}$	18.311	1.905	0.1391	0.469
		$d_{5/2}$	18.285	2.542	0.1853	0.521
		total		40.241	4.018	0.123
20	0.2719	$s_{1/2}$	23.653	9.970	1.153	3.24[−3]
		$p_{1/2}$	23.553	4.894	0.4253	0.231
		$p_{3/2}$	23.448	7.764	0.6814	0.243
		$d_{3/2}$	23.311	0.8875	0.05878	0.559
		$d_{5/2}$	23.285	1.168	0.07738	0.618
		total		24.68	2.396	0.126
50	0.4127	$s_{1/2}$	53.653	2.707	0.2675	8.30[−3]
		$p_{1/2}$	53.553	0.7866	0.04816	0.424
		$p_{3/2}$	53.448	1.122	0.06965	0.562
		$d_{3/2}$	53.311	0.0633	0.00269	1.000
		$d_{5/2}$	53.285	0.0786	0.00335	1.100
		total		4.758	0.3913	0.129

[a]2.15[−3] denotes 2.15×10^{-3}.

appear to be only mild variations in the angular factors with ion species.

Even in the few keV range there are noticeable relativistic effects. Their effects need to be taken into account in interpreting photoelectric experiments and a distinction must be made between angular correlation experiments carried out relative to the photon's direction and its polarization direction.

ACKNOWLEDGMENTS

The author wishes to thank the EBIT experimental group for discussions and Dr. Andrew Hazi for a critical reading. This work was performed under the auspices of the U.S. Department of Energy by the Lawrence Livermore National Laboratory under Contract Number W-7405-ENG-48.

[1]H. K. Tseng, R. H. Pratt, S. Yu, and A. Ron, Phys. Rev. A **17**, 1061 (1978); Y. S. Kim, R. H. Pratt, A. Ron, and H. K. Tseng, *ibid.* **22**, 567 (1980).

[2]See references in R. H. Pratt, Indian J. Phys. **58A**, 1 (1984).

[3]R. E. Marrs, M. A. Levine, D. A. Knapp, and J. R. Henderson, Phys. Rev. Lett. **60**, 1715 (1988).

[4]J. R. Henderson (private communication).

[5]E. B. Saloman, J. H. Hubbell, and J. H. Scofield, At. Data Nucl. Data Tables **38**, 1 (1987).

[6]R. H. Pratt, R. D. Levee, R. L. Pexton, and W. Aron, Phys. Rev. **134**, A898 (1964).

[7]W. R. Alling and W. R. Johnson, Phys. Rev. **139**, A1050 (1965).

[8]S. Hultberg, B. Nagel, and P. Olsson, Ark. Fys. **38**, 1 (1968).

[9]R. H. Pratt, A. Ron, and H. K. Tseng, Rev. Mod. Phys. **45**, 273 (1973).

[10]T. E. H. Walker and J. T. Waber, J. Phys. B **6**, 1165 (1973).

[11]R. M. Steffen and K. Alder, in *The Electromagnetic Interaction in Nuclear Spectroscopy,* edited by J. H. Hamilton (North-Holland, Amsterdam, 1975), Chap. 12, p. 505; J. H. Scofield, in *Atomic Inner-Shell Processes,* edited by B. Crasemann (Academic, New York, 1975), Vol. 1, p. 265.

[12]H. J. Rose and D. M. Brink, Rev. Mod. Phys. **39**, 306 (1967).

[13]J. H. Scofield, Phys. Rev. **179**, 9 (1969).